Electronic Supplementary Material (ESI) for Nanoscale.

Supporting Information

Interfacial N-Cu-S Coordination Mode of $CuSCN/C_3N_4$ with Enhanced Electrocatalytic Activity for Hydrogen Evolution

Ziming Zhao,[a] Haidong Yang,[b] Yan Zhu,[a] Sha Luo,[a] and Jiantai Ma*[a]

[a] State Key Laboratory of Applied Organic Chemistry (SKLAOC), The Key Laboratory of Catalytic Engineering of Gansu Province, College of Chemistry and Chemical Engineering, Lanzhou University, Lanzhou, Gansu, 730000, P. R. China

[b] Key Laboratory of Eco-Environment-Related Polymer Materials, Ministry of Education of China, Key Laboratory of Polymer Materials of Gansu Province, College of Chemistry and Chemical Engineering, Northwest Normal University, No. 967 Anning East Road, Lanzhou 730070, P.R. China

E-mail: majiantai@lzu.edu.cn

Experimental section:

1、 Estimation of electrochemically active surface areas (A_{echem})

Based on previous reports,[1, 2] cyclic voltammetry (CV) could be carried out in neutral media to probe the electrochemical double-layer capacitance (C_{dl}) of various samples at non-Faradaic overpotentials as the means for estimating the A_{echem} of samples. Accordingly, a series of CV measurements were performed at various scan rates (4 mV s^{-1}, 8 mV s^{-1}, 12mV s^{-1}, 16 mV s^{-1}, etc.) in 0.1 to 0.2 V vs. RHE range, and the sweep segments of the measurements were set to 10 to ensure consistency. By plotting the difference in current density (J) between the anodic and cathodic sweeps (J_{anodic} - $J_{cathodic}$) at 0.15 V vs. RHE against the scan rate, a linear trend was observed. The slope of the fitting line is found to be equal-to-twice the geometric C_{dl}, which is proportional to the A_{echem} of the materials. Therefore, the A_{echem} of different samples can be compared with one another based on their C_{dl} values. However, it should be noted that this comparison makes sense only when the measurements of materials were carried out under the same conditions.

2、 Measurements of electrochemical impedance spectroscopy (EIS)

EIS studies were performed under operating conditions (i.e., at a cathodic bias that drives rapid hydrogen evolution)[2] at -0.17 V vs. RHE with an applied sinusoidal voltage at amplitude of 5 mV while sweeping the frequency from 100 kHz to 0.01 Hz. The impedance data were then fitted, and the geometric values of series resistance (R_s) and charge transfer resistance (R_{ct}) were measured.

3、 TOF calculation

To calculate the per site turnover frequency (TOF), we used the following formula:[3, 4]

$$TOF = \frac{number\ of\ total hydrogen\ turnovers/cm^2\ of\ geometric\ area}{number\ of\ active\ sites/cm^2\ of\ geometric\ area}$$

The total number of hydrogen turnovers was calculated from the current density according to:

$$no.\ of\ H_2 =$$

$$\left(j\frac{mA}{cm^2}\right)\left(\frac{1C^{-1}}{1000\ mA}\right)\left(\frac{1\ mol\ of\ e^{-1}}{96485.3\ C}\right)\left(\frac{1\ mol\ of\ H_2}{2\ mol\ of\ e^{-}}\right)\left(\frac{6.022\ mol\ \times\ 10^{22}\ H_2\ moleculars}{1\ mol\ H_2}\right)$$

$$= 3.12 \times 10^{15}\frac{H_2/s}{cm^2}per\frac{mA}{cm^2}$$

Because the interfacial coordinated N-Cu-S can act as the catalytically active species for CuSCN/C_3N_4, therefore, the surface low-coordinated Cu ions of CuSCN were considered to be the catalytically active species for CuSCN/C_3N_4 and pure CuSCN. On the basis of the electrochemical active surface area together with the unit cell (volume of 139.87 Å^3) of the CuSCN crystal structure in the cases of CuSCN/C_3N_4 and pure CuSCN, a similar approach was used to estimate TOF for them. Active sites per real surface area:

$$Active\ sites_{CuSCN/C3N4} = Active\ sites_{CuSCN} = \left(\frac{2\ atom/unit\ cell}{139.87\ Å^3/unit\ cell}\right) = 5.89\ \times 10^{14} \times atoms\ cm^{-2}$$

$$TOF = \frac{(3.12 \times 10^{15}\frac{H_2/s}{cm^2}per\frac{mA}{cm^2}cm^2}{surface\ sites \times A_{echem}} \times |j|$$

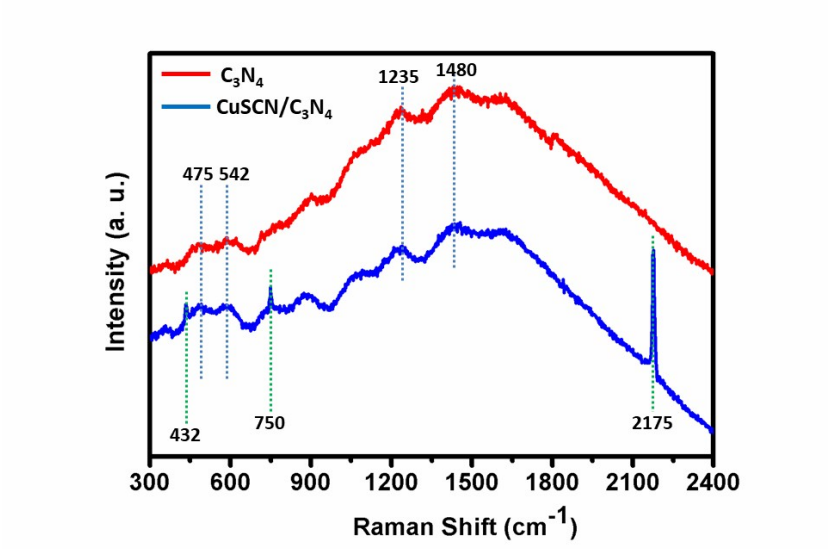

Figure S1. Raman spectra of C_3N_4 and CuSCN/C_3N_4

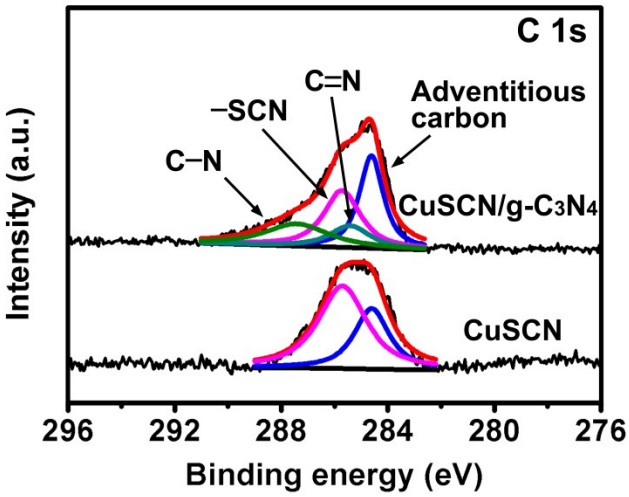

Figure S2. C 1s XPS spectra of $CuSCN/C_3N_4$ and pure CuSCN taken after synthesis.

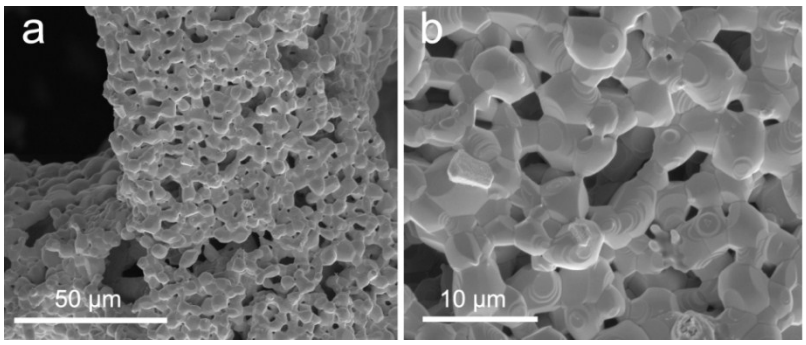

Figure S3. SEM images of pure CuSCN.

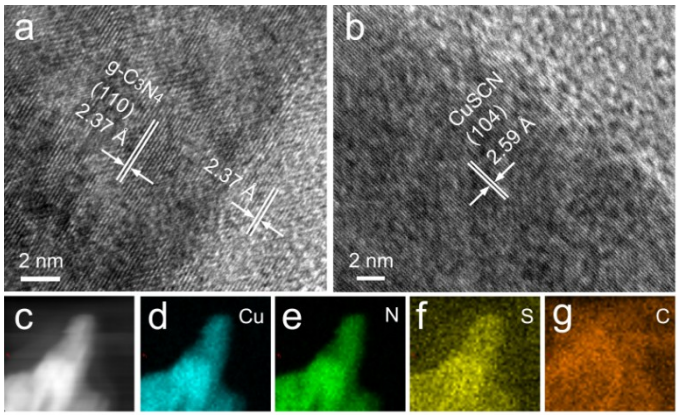

Figure S4. HRTEM images of a) $CuSCN/C_3N_4$ and b) pure CuSCN. c-g) elemental mappings of pure CuSCN.

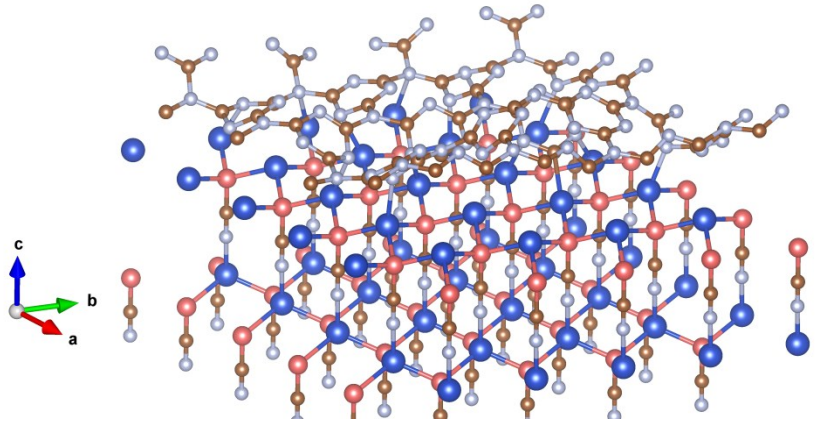

Figure S5. Optimized structure CuSCN coupled with one-layer C_3N_4 shell.

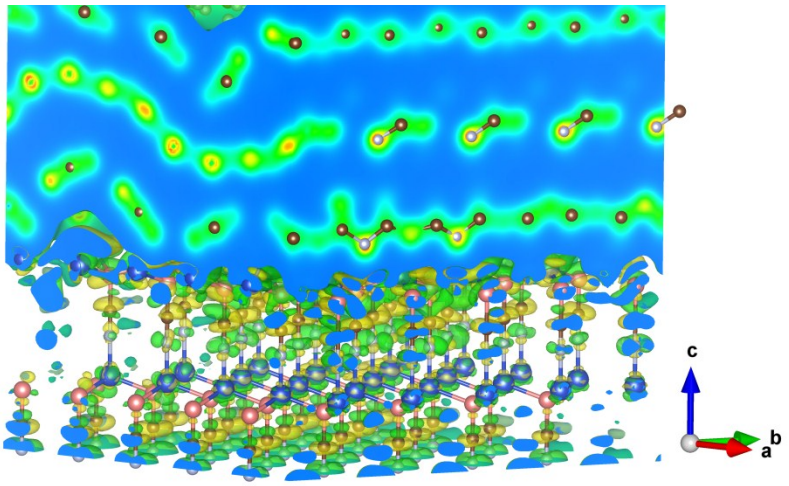

Figure S6. Calculated charge-density differences of CuSCN coupled with three-layer C_3N_4 shells. The isosurface value of the colour region is 0.6 e $Å^{-3}$. The green and yellow regions refer to increased and decreased charge distributions. Blue, red, brown and white represent Cu, S, C, and N atoms, respectively.

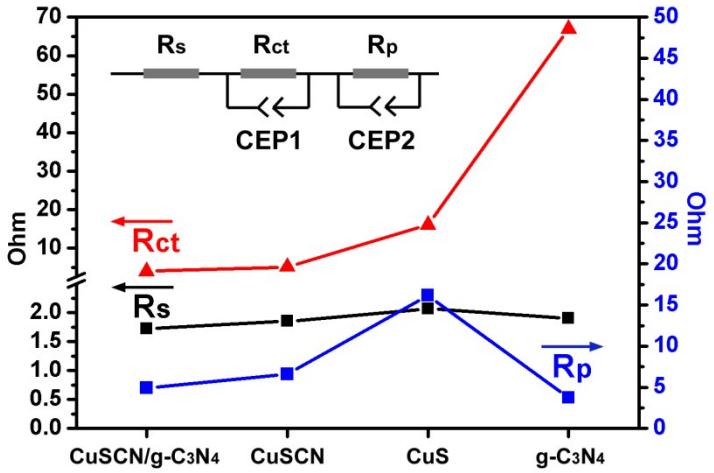

Figure S7. Electrical equivalent circuit model for fitting the EIS response of hydrogen evolution reaction on CuSCN/C_3N_4, pure CuSCN, CuS, and C_3N_4 electrodes, where R_s is series resistance, R_{ct} at low frequency denotes charge transfer resistance, R_p at high frequency region relates to the surface roughness of the material, and the double-layer capacitance (C_{dl}) is represented by the elements CPE1 and CPE2.

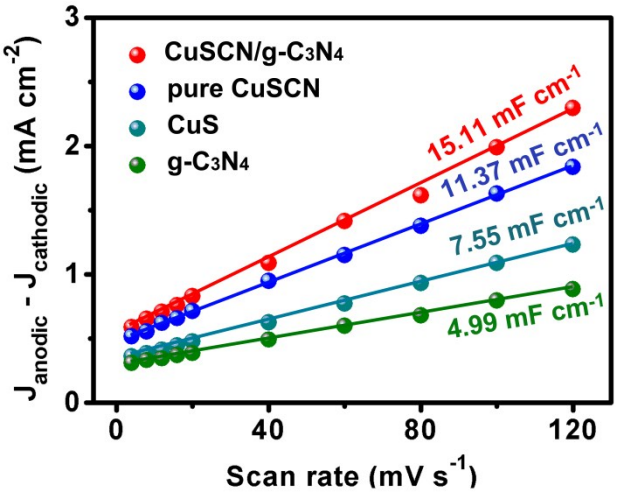

Figure S8. Plots used for evaluating the C_{dl} of CuSCN/C_3N_4, pure CuSCN, CuS and C_3N_4.

Table S1. Local structure parameters around Cu in samples estimated by EXAFS

analysis.

Catalyst	Shell	R(Å)[a]	N[b]	σ^2(10^{-3} Å^2)[c]	ΔE_0 [eV][d]
Pure CuSCN	Cu-N	1.91	1.0	8.1	0.93
	Cu-S	2.31	3.0	4.9	1.2
CuSCN/C_3N_4	Cu-N	2.07	1.1	8.3	1.6
	Cu-S	2.29	3.0	4.6	2.7

[a] R = distance between absorber and backscatter atoms; [b] N = coordination number; [c] σ^2 = Debye-Waller factor; [d] ΔE_0 = energy shift.

Table S2. Comparison of the electrocatalytic performance of CuSCN/C_3N_4 versus HER electrocatalysts reported recently.

Catalyst	Electrolyte Solution	Current Density (j)	Overpotential at the Corresponding j	Stability	Reference
CuSCN/C_3N_4	0.5 M H_2SO_4	10 mA/cm^2	85 mV	20 h	This work
CuCo@NC	0.5 M H_2SO_4	10 mA/cm^2	145 mV	8 h	[5]
NiCu@C	0.5 M H_2SO_4	10 mA/cm^2	48 mV	3.3 h	[6]
Cu-CMP	1 M KOH	1 mA/cm^2	190 mV	_	[7]
CFP/$NiCo_2O_4$/CuS	0.5 M H_2SO_4	10 mA/cm^2	72.3 mV	50 h	[8]
Cu_7S_4@MoS_2	0.5 M H_2SO_4	10 mA/cm^2	133 mV	10 h	[9]
Cu_3P NW/CF	0.5 M H_2SO_4	10 mA/cm^2	143 mV	25 h	[10]
Cu NDs/Ni_3S_2 NTs-CFs	1 M KOH	10 mA/cm^2	128 mV	30 h	[11]
Cu/Cu_2O	0.5 M KPi	8 mA/cm^2	~320 mV	_	[12]

Cu@NiFe LDH	1M KOH	10 mA/cm^2	116 mV	48 h	[13]
Cu@CoSx/CF	1M KOH	10 mA/cm^2	134 mV	200 h	[14]
N,P-doped GO	0.5 M H_2SO_4	30 mA/cm^2	210 mV	4 h	[15]
N,S-doped graphene	0.5 M H_2SO_4	10 mA/cm^2	276 mV	_	[16]
C_3N_4@N-doped graphene	0.5 M H_2SO_4	10 mA/cm^2	240 mV	_	[17]
TiO_2 NDs/Co NSNTs-CFs	1.0 M KOH	10 mA/cm^2	108 mV	100 h	[18]
Mn doped $CoSe_2$	0.5 M H_2SO_4	10 mA/cm^2	~190 mV	17 h	[19]

Table S3. The TOF values of CuSCN/C_3N_4 and pure CuSCN at the overpotential of 0.2 V vs. RHE.

Sample	**TOF (s-1)**
CuSCN/C_3N_4	6.35
Pure CuSCN	1.36

Table S4. The ICP-OES measured values of Cu content for CuSCN/C_3N_4 and pure CuSCN in 0.5 M H_2SO_4 electrolyte after the chronoamperometric measurement for a 5, 10, and 20 h period.

Period	**Cu content in electrolyte for CuSCN/C_3N_4**	**Cu content in electrolyte for pure CuSCN**
5 h	0.1 mg	0.7 mg

10 h	0.1 mg	2.1 mg
20 h	0.2 mg	2.3 mg

References

1 J. Xie, S. Li, X. Zhang, J. Zhang, R. Wang, H. Zhang, B. Pan, Y. Xie, *Chem. Sci.*, 2014, **5**, 4615-4620.

2 L. Feng, G. Yu, Y. Wu, G. Li, H. Li, Y. Sun, T. Asefa, W. Chen, X. Zou, *J. Am. Chem. Soc.*, 2015, **137**, 14023-14026.

3 R. Kötz, M. Carlen, *Electrochim. Acta*, 2000, **45**, 2483-2498.

4 X. Wang, Y. Xu, H. Rao, W. Xu, H. Chen, W. Zhang, D. Kuang, C. Su, *Energy Environ. Sci.*, 2016, **9**, 1468-1475.

5 M. Kuang, Q. Wang, P. Han, G. Zheng, *Adv. Energy Mater.*, 2017, **7**, 1700193.

6 Y. Shen, Y. Zhou, D. Wang, X. Wu, J. Li, J. Xi, *Adv. Energy Mater.*, 2017, **7**, 1701759.

7 S. Cui, M. Qian, X. Liu, Z. Sun, P. Du, *ChemSusChem,* 2016, **9**, 2365-2373.

8 L. An, L. Huang, P. Zhou, J. Yin, H. Liu, P. Xi, *Adv. Funct. Mater.*, 2015, **25**, 6814-6822.

9 J. Xu, J. Cui, C. Guo, Z. Zhao, R. Jiang, S. Xu, Z. Zhuang, Y. Huang, L. Wang, Y. Li, *Angew. Chem. Int. Ed.*, 2016, **55**, 6502- 6505.

10 J. Tian, Q. Liu, N. Cheng, A. M. Asiri, X. Sun, *Angew. Chem. Int. Ed.*, 2014, **53**, 9577-9581.

11 J. Feng, J. Wu, Y. Tong, G. Li, *J. Am. Chem. Soc.*, 2018, **140**, 610-617.

12 J. Zhao, P. D. Tran, Y. Chen, J. S. C. Loo, J. Barber, Z. J. Xu, *ACS Catal.*, 2015, **5**, 4115-4120.

13 L. Yu, H. Zhou, J. Sun, F. Qin, F. Yu, J. Bao, Y. Yu, S. Chen, Z. Ren, *Energy Environ. Sci.*, 2017, **10**, 1820-1827.

14 Y. Liu, Q. Li, R. Si, G. Li, W. Li, D. Liu, D. Wang, L. Sun, Y. Zhang, X. Zou, *Adv. Mater.*, 2017, **29**, 1606200.

15 J. Zhang, L. Qu, G. Shi, J. Liu, J. Chen, L. Dai, *Angew. Chem. Int. Ed.*, 2016, **55**, 2230-2234.

16 Y. Ito, W. Cong, T. Fujita, Z. Tang, M. Chen, *Angew. Chem. Int. Ed.*, 2015, **54**, 2131-2136.

17 Y. Zheng, Y. Jiao, Y. Zhu, L. Li, Y. Han, Y. Chen, A. Du, M. Jaroniec, S. Qiao, *Nature Commun.*, 2014, **5**, 3783.

18 J. Feng, H. Xu, Y. Dong, X. Lu, Y. Tong, G. Li, *Angew. Chem. Int. Ed.*, 2017, **56**, 2960-2964.

19 Y. Liu, X. Hua, C. Xiao, T. Zhou, P. Huang, Z. Guo, B. Pan, Y. Xie, *J. Am. Chem. Soc.*, 2016, **138**, 5087-5092.